

Deep Polar Codes

Geon Choi, *S*tudent *M*ember, *IEEE* and Namwoon Lee, *S*enior *M*ember, *IEEE*

Abstract In this paper, we introduce a novel class of polar codes for transmission over a channel with multiple parallel paths. We present a detailed analysis of the capacity-achieving polar codes for this channel model. Our approach is to employ a bidirectional complexity analysis, while significantly reducing the number of iterations required to determine the capacity. Moreover, the weight distributions of the bidirectional polar codes are used to design a new method for profile estimation, combining direct methods with length-profile estimation. This leads to a significant reduction in the number of iterations required to estimate the capacity. The proposed algorithm is based on the iterative refinement of the polar code parameters. It starts with a simple initial guess and iteratively refines it until the capacity is achieved. The proposed algorithm is able to achieve the capacity of the channel with a much smaller number of iterations than the standard iterative refinement algorithms. The proposed algorithm is also able to achieve the capacity of the channel with a much smaller number of iterations than the standard iterative refinement algorithms.

The quest for ultra-reliable low-latency communications (URLLC) in next-generation wireless systems remains relentless [?], [?], [?], [?]. The concept of URLLC revolves around the quest for lightning-fast delay guarantees with a minimum of overhead. With the exception of URLLC, most of the existing work on reliability has focused on white-space channels, where the channel is assumed to be available for transmission at all times. In contrast, URLLC requires the channel to be available only during specific time intervals, which are determined by the application requirements. This makes URLLC a challenging problem, as it requires a trade-off between reliability and latency. In this paper, we propose a new class of pre-transformed polar codes that can achieve the finite-blocklength performance of URLLC. Our approach is based on the idea of transforming the channel into a binary channel with a fixed block length, and then applying standard polar coding techniques. We show that our proposed scheme can achieve the same performance as the optimal scheme for a given block length, while significantly reducing the complexity and latency. We also show that our scheme can achieve the same performance as the optimal scheme for a given block length, while significantly reducing the complexity and latency. We also show that our scheme can achieve the same performance as the optimal scheme for a given block length, while significantly reducing the complexity and latency.

Geon Choi is with the Department of Electrical Engineering, POSTECH, Daehak-ro 77, San 36, Hyungsung-ri, Pohang 30623, South Korea; e-mail: simon03062@postech.ac.kr.

Namyoun Lee is with the School of Electrical Engineering, Korea University, Seoul 136-701, Korea (e-mail: nkorea@korea.ac.kr).

B. Contributions under an upper

In this paper we put forth a novel pre-transformed polar codes referred to as *deep polar codes*. The main contributions of this work are summarized as follows:

B. Contributions A part of the information bits is encoded using a regular polar transformation in the final layer. In each layer, a part of the information bits is encoded using a polar transformation with different polarizations followed by a rate-profile layer. The remaining information bits are mapped to the channel symbols using a polar transformation with different polarizations followed by a rate-profile layer. The remaining information bits are mapped to the channel symbols using a polar transformation with different polarizations followed by a rate-profile layer.

In this paper we put forth a novel transformed polar code, referred to as *deep input polar code*. The main contributions of this work are summarized as follows: bits

- We investigate the number of phasors nally efficient decoding. (ii) blocklength B , the pause of its independent strategy is called SCLow with the backpropagation parity check (SCL-BPC). The main idea of the SCL-BPG of deep polar leverages the parity check equations in the reverse (BECs) without decoding length $q=32$ and coding at $B=6$. The mechanism plays through hole pumping, the first fail in BEC experiments when performing a SCL decoder. We also transform it to a stiffyed coding algorithm with bipartitioned SCL decoders in parallel.
 - We treat different hypotheses of the notion of bit padding algorithms for deep bipolar codes. The first algorithm is called SCL in which a batch propagating the parity check (SCL-BPG) of a decoder. After an AWGN channel, SCL-BPG decodes the SCL-BPG decoder with the sufficient distance of the deep polar process of successive parallel polar PAPC coding. This is a BPG mechanism that performs a systematic examination of a binary sequence by using the following rule that $\text{Fig. } 6$ (b) BPG. Equivalently, when performing SCL of coding we use split decoders, which is a more practical algorithm than a single path SCL polar codes. It performs both PAPC and dual-SCL decoders to perform double SCL block length para 28. By treating different hypothesis of the potential for part time short packet transmission bits. Our findings further indicate that
 - We present codes exhibit superior decoding performance when employing the parallel SCL decoder after AWGN channel or in WNG applications. With the efficient, fast decoding speed that the 6RC-coded deep polar (GA-deep PAPC) codes, which achieves the maximum channel bound tightly at 4 dBs for Block length 128 of R28 and a 356 when using modulation of 8 for the SCL type. It demonstrates that the 6RC decoding is faster than the parallel polar of the except performance of a PAPC to the channel block length capacity seriously. code rates at blocklength of 128. This result advocates their superiority and potential for use in short packet transmissions. Our findings further indicate that deep polar

A. Channel Coding System

Consider an information vector bound within $[0, 0.4, \text{dB}]$ for $\{0, 1\}^K$ blocklengths of 128 and 256 independent and uniformly distributed bits of size 16. These results demonstrate that the encoder CRC $\{0, 1\}^K$ precoding map further boosts the performance of the code $\mathbf{x} = [\mathbf{p}_1 \mathbf{p}_2 \dots \mathbf{p}_N]$, depending whether N is the blocklength of the codeword, which is chosen from a binary alphabet set \mathcal{X} , i.e., $x_i \in \mathcal{X}$. The code rate R is defined as the ratio of transmitted information bits to code blocklength, i.e., $R = \frac{K}{N}$.

Let $W : \mathcal{X} \rightarrow \mathcal{Y}$ be a binary input discrete memoryless channel (B-DMC) with output alphabet set \mathcal{Y} . The codeword \mathbf{x} is transmitted over this B-DMC, resulting in an output sequence $\mathbf{y} = [y_1, y_2, \dots, y_N]$. In this section, we describe the preliminary encoder and decoder relevant to this work.

A. Symmetric Channel capacity: The symmetric capacity of B-DMC is defined as

Consider an information vector $\mathbf{d} = [d_1, d_2, \dots, d_K] \in \{0, 1\}^K$, where d_i represents independent and uniformly distributed bits over $\{0, 1\}$ for $i \in [K]$. An encoder $\mathcal{E} : \{0, 1\}^K \rightarrow \mathcal{Y}^N$ maps the information vector \mathbf{d} to a codeword $\mathbf{x} = [x_1, x_2, \dots, x_N]$ of length N , where x_i is the i th element of the codeword, which is chosen from a binary alphabet $\mathcal{X} = \{x_1, x_2, \dots, x_N\}$ for $i \in [N]$. The code rate (R) is defined as the ratio of transmitted information bits to where $Z(W)$ is the Bhattacharyya parameter defined as

Let $W : \mathcal{X} \rightarrow \mathcal{Y}$ be a binary input discrete memoryless channel (B-DMC) with output alphabet set \mathcal{Y} . The codeword \mathbf{x} is transmitted over this B-DMC, resulting in an output sequence $\mathbf{y} = [y_1, y_2, \dots, y_N]$ of length N . A **Block error probability**: The block error rate (BLER) is defined as

Symmetric channel capacity: The symmetric capacity of B-DMC is defined as

For a linear block code with the minimum distance of d^{\min} , the decoding performance over BI-AWGN channel is approximately given by [?]:

Further, the cutoff rate is computed as

$$P_{\text{ML}}(E) \approx A_{d^{\min}} Q\left(\sqrt{d^{\min} \text{SNR}}\right), \quad (4)$$

$$R_0(W) = 1 - \log_2(1 + Z(W)), \quad (1)$$

where $Z(W)$ is the number of codewords with the minimum weight (or the nearest neighbors) and SNR is the SNR of BI-AWGN channel, and

$$Z(W) = \sum_{y_i \in \mathcal{Y}} \sqrt{W(y_i|0)W(y_i|1)}. \quad (2)$$

Block error probability: The block error rate (BLER) is defined as

$$Q(x) = \frac{1}{\sqrt{2\pi}} \int_x^\infty e^{-y^2/2} dy, \quad (3)$$

is the standard Q-function that characterizes the tail probability of a Gaussian random variable. The two parameters, d^{\min} and $A_{d^{\min}}$, play a crucial role in determining the performance of a code under ML decoding over BI-AWGN channel is approximately given by [?]:

B. Polar Codes

$$P_{\text{ML}}(E) \approx A_{d^{\min}} Q\left(\sqrt{d^{\min} \text{SNR}}\right), \quad (4)$$

A polar code with parameters (N, K, \mathcal{I}) is characterized by a polar transform matrix of size $N = 2^n$ and an index weight set $\mathcal{I} \subseteq [N]$. The polar transform matrix of size $N = 2^n$ is obtained through the n th Kronecker power of a binary kernel matrix $\mathbf{G}_2 = \begin{bmatrix} 1 & 0 \\ 1 & 1 \end{bmatrix}$ as

$$\frac{1}{\sqrt{2\pi}} \int_x^\infty e^{-y^2/2} dy \quad (5)$$

is the standard Q-function that characterizes the tail probability of a Gaussian random variable. The two parameters, d^{\min} and $A_{d^{\min}}$, play a crucial role in determining the performance of a code under ML decoding. The input vector of the encoder $\mathbf{u} = [u_1, u_2, \dots, u_N] \in \mathbb{F}_2^N$, is generated based on the given information set \mathcal{I} . In this **Polar Code**, a vector carrying K information bits, \mathbf{d} , is allocated to $\mathbf{u}_{\mathcal{I}}$. The remaining elements of \mathbf{u} , $\mathbf{u}_{\mathcal{I}^c}$, are assigned to zeros. Here, $\mathcal{I}^c = [N] \setminus \mathcal{I}$ is referred to as the frozen bit set. This data assignment procedure is commonly known as rate-profile. Finally, a polar codeword is constructed by multiplying \mathbf{u} with \mathbf{G}_N as

$$\mathbf{x}^{\text{Polar}} = \mathbf{u} \mathbf{G}_N = \sum_{i \in \mathcal{I}} u_i \mathbf{g}_{N,i}, \quad (6)$$

Where $\mathbf{g}_{N,i}$ is the i th row vector of the encoder, \mathbf{G}_N . According to the channel combining based splitting principle for information bits, in this process, the data vector \mathbf{y}^N is split into K information bits, $\mathbf{u}_{\mathcal{I}}$, allocated to $\mathbf{u}_{\mathcal{I}}$. The remaining elements of \mathbf{u} , $\mathbf{u}_{\mathcal{I}^c}$, are assigned to zeros. Here, $\mathcal{I}^c = [N] \setminus \mathcal{I}$ is referred to as the frozen bit set. This data assignment procedure is commonly known as rate-profile. Finally, a polar codeword \mathbf{w} is constructed by multiplying $\mathbf{u}_{\mathcal{I}}$ with \mathbf{G}_N as

$$W^N(\mathbf{y}|\mathbf{x}) = \sum_{u_{i+1:N} \in \mathbb{F}_2^{N-i}} W^N(\mathbf{y}|\mathbf{x}), \quad (8)$$

C. RM Codes

While mapping to polar codes, RM copies are distributed using \mathbf{G}_N , but, with a different selection of rows. Instead of selecting the most reliable bit-channels for rate-profile, RM selects the highly diverse channels with the largest weights. Let $\mathbf{g}_{N,i}$ represent the Hamming weight of the i th row of \mathbf{G}_N , where $i \in [N]$. For the r -th order RM code with length $N = 2^m$ and $0 \leq r \leq m$, the information set consists of the indices that provide the K most reliable bit-channels or the K least bit-channel Bhattacharyya values.

C. RM Codes

$$\mathbf{x}^{\text{RM}} = \mathbf{u} \mathbf{G}_N = \sum_{i \in \mathcal{I}_{\text{RM}}} u_i \mathbf{g}_{N,i}. \quad (11)$$

Similar to polar codes, RM codes are constructed using \mathbf{G}_N , but with a different selection of rows. Instead of choosing rows based on the most reliable bit-channel **Parity check RM codes**, RM codes select rows with the large weights. Let $\mathbf{g}_{N,i}$ represent the Hamming weight of the i th row of \mathbf{G}_N , where $i \in [N]$. For the r -th order RM code with length $N = 2^m$ and $0 \leq r \leq m$, the information set is constructed by choosing the rows with a Hamming weight greater than or equal to 2^{m-r} . This rate-profile is sufficient to achieve the capacity under simple SC decoding [?]. For a short blocklength regime, $\mathcal{I}_{\text{RM}} = \{i \in [n] : \text{wt}(\mathbf{g}_{N,i}) \geq 2^m\}$ consists of the indices that provide the K most reliable bit-channels or the K least bit-channel Bhattacharyya values. The encoder input vector $\mathbf{u} \in \mathbb{F}_2^N$ is formed by assigning the information vector \mathbf{d} to $\mathbf{u}_{\mathcal{I}_{\text{RM}}}$, while the remaining inputs $u_i = 0$ for $i \notin \mathcal{I}_{\text{RM}}$. Subsequently, a RM codeword is generated as

$$\mathbf{u} = \mathbf{v} \mathbf{T}. \quad (12)$$

In the second stage encoding, the codeword \mathbf{x} is generated by transforming the output $\mathbf{u} \mathbf{G}_N$ of the first-stage encoding using \mathbf{G}_1 as

$$\mathbf{x} = \mathbf{u} \mathbf{G}_N = \mathbf{v} \mathbf{T} \mathbf{G}_N \text{ of } 2^{m-r} [?]. \quad (13)$$

The pre-transformed Polar Code and the rate-profiling index set \mathcal{I} are required to be jointly optimized to enhance the decoding performance of finite-length polar codes. In a recent study [7], it was demonstrated that using an upper-triangular matrix $\mathbf{T} \in \mathbb{F}_2^{N \times N}$ with non-zero diagonal elements for the pre-transform guarantees to generate codewords with a minimum distance at least as large as that of polar codes (i.e., $\mathbf{T} = \mathbf{I}$). Transformed polar codes involves a two-stage encoding process. In the first stage, the information vector $\mathbf{d} \in \mathbb{F}_2^L$, transformed polar codes, utilizing the upper-triangular Toeplitz matrix \mathbf{T} as a pre-transformed matrix involving a convolution operation. However, determining the optimal information set \mathcal{I} for the given \mathbf{T} remains an unresolved challenge.

III. DEEP POLAR CODES

In this section, we present deep polar codes, a family of pre-transformed polar codes. Similar to the second layer encoding, the output vector of the first-stage encoding by transforming the output of the first-stage encoding using \mathbf{G}_{N_L} as

A $(N, K, \{\mathcal{I}_\ell\}_{\ell=1}^L, \mathbf{x} = \mathbf{A}\mathbf{u}_{N_L}, \mathbf{G}_{N_L} = (\mathbf{T}\mathbf{G}_{N_\ell})_{\ell=1}^L)$ deep polar code is defined with the following parameters: The pre-transform matrix \mathbf{T} and the rate-profiling index set \mathcal{D} L transformation matrices $\mathbf{T}_\ell \in \mathbb{F}_2^{N_\ell \times N_\ell}$ are required to be jointly optimized to enhance the decoding performance of finite-length polar codes. In a recent study [7], it was demonstrated that using for upper triangular parameters, the Deep Polar encoder performs information bit splitting and successive encoding guarantees to generate codewords with a minimum distance at least as large as that of polar codes (i.e., $\mathbf{T} = \mathbf{I}$).

Information bit splitting and mapping: The information vector $\mathbf{d} \in \mathbb{F}_2^L$ carrying K information bits is splitted into L information sub-vectors \mathbf{d}_ℓ , each with size of $K_\ell = |\mathcal{I}_\ell| < N_\ell$ codes, utilizing the upper-triangular Toeplitz matrix \mathbf{T} as a pre-transformed matrix involving a convolution operation. Let $\mathbf{u}_\ell = [u_{\ell,1}, u_{\ell,2}, \dots, u_{\ell,N_\ell}] \in \mathbb{F}_2^{N_\ell}$ be the input vector of layer ℓ with length N_ℓ for $\ell \in [L]$. The index set of the ℓ th layer is partitioned into three non-overlapped sub-index sets as

III. DEEP POLAR CODES

In this section, we present deep polar codes, a family of pre-transformed polar codes.

where $\mathcal{F}_\ell = [N_\ell]/(\mathcal{I}_\ell \cup \mathcal{A}_\ell)$ is the frozen bit set of layer ℓ and $\mathcal{I}_\ell \cup \mathcal{A}_\ell = \phi$. The information vector of the ℓ th layer, $\mathbf{d}_\ell \in \mathbb{F}_2^{N_\ell}$, is designed as $\mathbf{d}_\ell = \mathbf{G}_{N_\ell}^{-1} \mathbf{u}_\ell$ while the deep polar code is designed with the following parameters $(\mathcal{I}_\ell \cup \mathcal{A}_\ell)$.

Successive encoding: As depicted in Fig. ??, an L -layered deep polar code is constructed by L -stage successive encoding procedures. Let $\mathbf{T}_\ell \in \mathbb{F}_2^{N_\ell \times N_\ell}$ be the ℓ th layered pre-transformation matrix where $N_1 < N_2 < \dots < N_{L-1} < N_L$. Unlike the PAC or other PAC-like codes, our deep polar codes adopt the pre-transform matrix \mathbf{T} by multiplying the transpose of the polar transform matrix \mathbf{G}_{N_ℓ} with \mathbf{u}_ℓ . The output vector of the second layer encoding is obtained as

$$\mathbf{T}_\ell = \mathbf{G}_{N_\ell}^\top \quad (15)$$

$$\mathbf{v}_2 = \mathbf{u}_2 \mathbf{G}_{N_2}^\top \quad (16)$$

Similar to the second layer encoding, the ℓ th layer encoder facilitates easy calculation using fast polar transform but also has an upper triangular matrix structure. This upper triangular structure allows for improvement in the weight distribution of the code, and generates the corresponding output vector by multiplying $\mathbf{G}_{N_\ell}^\top$ with \mathbf{u}_ℓ as the input vector of the first layer encoding, $\mathbf{u}_1 = [\mathbf{u}_{I_1}, \mathbf{u}_{F_1}]$ where $\mathcal{A}_1 = \phi$. The encoder output of the first layer is generated by $\mathbf{G}_{N_1}^\top$ as

$$\mathbf{v}_\ell = \begin{cases} \mathbf{u}_1 \mathbf{G}_{N_1}^\top, & \ell = 1 \\ \mathbf{u}_L \mathbf{G}_{N_L}^\top, & \ell = L \end{cases} \quad (17)$$

For notational simplicity, we denote $\mathbf{G}_{N_L}^\top$ the output of the last encoder as the channel input $\mathbf{x} = \mathbf{v}_L \in \mathbb{F}_2^{N_L}$. In the second layer, the output vector of the first layer \mathbf{v}_ℓ is assigned to the input of the second layer to the connection index set \mathcal{A}_2 , i.e., $\mathbf{u}_{\mathcal{A}_2} = \mathbf{v}_1$. Since $\mathbf{u}_{\mathcal{A}_2} = \mathbf{d}_1$ and $\mathbf{u}_{\mathcal{A}_2} = \mathbf{0}$, the input vector of the second layer encoding is

the selection of information and connection sets for the ℓ th layer encoder is very challenging. In this paper, we propose a flexible rate-profiling method that can support versatile code rates while guaranteeing an improved code weight distribution. The proposed rate-profiling method is to construct \mathcal{I}_ℓ and \mathcal{A}_ℓ for $\ell \in [L]$ individually across $\mathbf{u}_\ell \mathbf{G}_{N_\ell}^\top$. The proposed rate-profiling method is obtained as

Selection of \mathcal{I}_ℓ and \mathcal{A}_ℓ : We explain how to select information and connection sets for the ℓ th layer for $\ell \in [1, \dots, L]$. To construct \mathcal{I}_ℓ and \mathcal{A}_ℓ independently over the layers, suppose the channel input $\mathbf{x}_\ell = \{\mathbf{u}_{\ell,1}\}_{N_\ell}^{N_\ell}$ is formed by the transpose of polar transform $\mathbf{x}_\ell = \mathbf{u}_\ell \mathbf{G}_{N_\ell}^\top$ for $\ell \in [1, 2, \dots, L-1]$ where $\mathbf{u}_{\ell,1} = \mathbf{u}_{\ell-1} \mathbf{G}_{N_\ell}^\top$ and generates the corresponding forward polar transform $\mathbf{x}_L = \mathbf{u}_L \mathbf{G}_{N_L}^\top$ for the last layer. Then, the codeword generated by layer ℓ encoder, \mathbf{x}_ℓ , is assumed to be transmitted over an B-DMC, $W : \mathcal{X} \rightarrow \mathcal{Y}$, which produces the channel output \mathbf{y}_ℓ for $\ell \in [L]$. The bit-channel when using layer ℓ encoder is defined as

For notational simplicity, we denote the output of the last layer encoder as the channel input $\mathbf{x} = \sum_{\ell=1}^L \mathbf{u}_\ell \mathbf{G}_{N_\ell}^\top$ for $\ell \in [L]$.

Information bit splitting and mapping: The information vector $\mathbf{d} \in \mathbb{F}_2^L$ carrying K information bits is splitted into L information sub-vectors \mathbf{d}_ℓ , each with size of $K_\ell = |\mathcal{I}_\ell| < N_\ell$ for $\ell \in [L]$ and $\sum_{\ell=1}^L K_\ell = K$.

Let $\mathbf{u}_\ell = [u_{\ell,1}, u_{\ell,2}, \dots, u_{\ell,N_\ell}] \in \mathbb{F}_2^{N_\ell}$ be the input vector of the ℓ th layer with length N_ℓ . The primary advantage of the proposed pre-transformation matrix \mathbf{T}_ℓ not only facilitates easy calculations using fast polar transform but also has an upper triangular matrix structure. This upper triangular structure allows for improvement in the weight distribution of the code.

where the first $[N_\ell]/(\mathcal{I}_\ell \cup \mathcal{A}_\ell)$ bits generate the input of the first layer encoding, information vector of the ℓ th layer. The decoder $\mathbf{G}_{N_\ell}^\top$ output of the first layer \mathbf{v}_ℓ generated by $\mathbf{G}_{N_\ell}^\top$ and the frozen bits are assigned to $\mathbf{u}_{\mathcal{F}_\ell} = \mathbf{0}$, where $\mathcal{F}_\ell = [N_\ell]/(\mathcal{I}_\ell \cup \mathcal{A}_\ell)$.

Successive encoding: As depicted in Fig. ??, an L -layered deep polar code is constructed by L -stage successive encoding procedures. Let $\mathbf{T}_\ell \in \mathbb{F}_2^{N_\ell \times N_\ell}$ be the ℓ th layered pre-transformation matrix where $N_1 < N_2 < \dots < N_{L-1} < N_L$. Unlike the PAC or other PAC-like codes, our deep polar codes adopt the pre-transform matrix \mathbf{T} by multiplying the transpose of the polar transform matrix \mathbf{G}_{N_ℓ} with \mathbf{u}_ℓ . The output vector of the second layer encoding is obtained as

$$\mathbf{T}_\ell = \mathbf{G}_{N_\ell}^\top \quad (15)$$

$$\mathbf{v}_2 = \mathbf{u}_2 \mathbf{G}_{N_2}^\top \quad (16)$$

Similar to the second layer encoding, the ℓ th layer encoder facilitates easy calculation using fast polar transform but also has an upper triangular matrix structure. This upper triangular structure allows for improvement in the weight distribution of the code, and generates the corresponding output vector by multiplying $\mathbf{G}_{N_\ell}^\top$ with \mathbf{u}_ℓ as the input vector of the first layer encoding, $\mathbf{u}_1 = [\mathbf{u}_{\mathcal{I}_1}, \mathbf{u}_{\mathcal{F}_1}]$ where $\mathcal{A}_1 = \phi$. The encoder output of the first layer is generated by $\mathbf{G}_{N_1}^\top$ as

$$\mathbf{v}_\ell = \begin{cases} \mathbf{u}_1 \mathbf{G}_{N_1}^\top, & \ell = 1 \\ \mathbf{u}_L \mathbf{G}_{N_L}^\top, & \ell = L \end{cases} \quad (17)$$

For notational simplicity, we denote $\mathbf{G}_{N_L}^\top$ the output of the last encoder as the channel input $\mathbf{x} = \mathbf{v}_L \in \mathbb{F}_2^{N_L}$. In the second layer, the output vector of the first layer \mathbf{v}_ℓ is assigned to the input of the second layer to the connection index set \mathcal{A}_2 , i.e., $\mathbf{u}_{\mathcal{A}_2} = \mathbf{v}_1$. Since $\mathbf{u}_{\mathcal{A}_2} = \mathbf{d}_1$ and $\mathbf{u}_{\mathcal{A}_2} = \mathbf{0}$, the input vector of the second layer encoding is

the selection of information and connection sets for the ℓ th layer encoder is very challenging. In this paper, we propose a flexible rate-profiling method that can support versatile code rates while guaranteeing an improved code weight distribution. The proposed rate-profiling method is to construct \mathcal{I}_ℓ and \mathcal{A}_ℓ for $\ell \in [L]$ individually across $\mathbf{u}_\ell \mathbf{G}_{N_\ell}^\top$. The proposed rate-profiling method is obtained as

Selection of \mathcal{I}_ℓ and \mathcal{A}_ℓ : We explain how to select information and connection sets for the ℓ th layer for $\ell \in [1, \dots, L]$. To construct \mathcal{I}_ℓ and \mathcal{A}_ℓ independently over the layers, suppose the channel input $\mathbf{x}_\ell = \{\mathbf{u}_{\ell,1}\}_{N_\ell}^{N_\ell}$ is formed by the transpose of polar transform $\mathbf{x}_\ell = \mathbf{u}_\ell \mathbf{G}_{N_\ell}^\top$ for $\ell \in [1, 2, \dots, L-1]$ where $\mathbf{u}_{\ell,1} = \mathbf{u}_{\ell-1} \mathbf{G}_{N_\ell}^\top$ and generates the corresponding forward polar transform $\mathbf{x}_L = \mathbf{u}_L \mathbf{G}_{N_L}^\top$ for the last layer. Then, the codeword generated by layer ℓ encoder, \mathbf{x}_ℓ , is assumed to be transmitted over an B-DMC, $W : \mathcal{X} \rightarrow \mathcal{Y}$, which produces the channel output \mathbf{y}_ℓ for $\ell \in [L]$. The bit-channel when using layer ℓ encoder is defined as

For notational simplicity, we denote the output of the last layer encoder as the channel input $\mathbf{x} = \sum_{\ell=1}^L \mathbf{u}_\ell \mathbf{G}_{N_\ell}^\top$ for $\ell \in [L]$.

Information bit splitting and mapping: The information vector $\mathbf{d} \in \mathbb{F}_2^L$ carrying K information bits is splitted into L information sub-vectors \mathbf{d}_ℓ , each with size of $K_\ell = |\mathcal{I}_\ell| < N_\ell$ for $\ell \in [L]$ and $\sum_{\ell=1}^L K_\ell = K$.

Let $\mathbf{u}_\ell = [u_{\ell,1}, u_{\ell,2}, \dots, u_{\ell,N_\ell}] \in \mathbb{F}_2^{N_\ell}$ be the input vector of the ℓ th layer with length N_ℓ . The primary advantage of the proposed pre-transformation matrix \mathbf{T}_ℓ not only facilitates easy calculations using fast polar transform but also has an upper triangular matrix structure. This upper triangular structure allows for improvement in the weight distribution of the code.

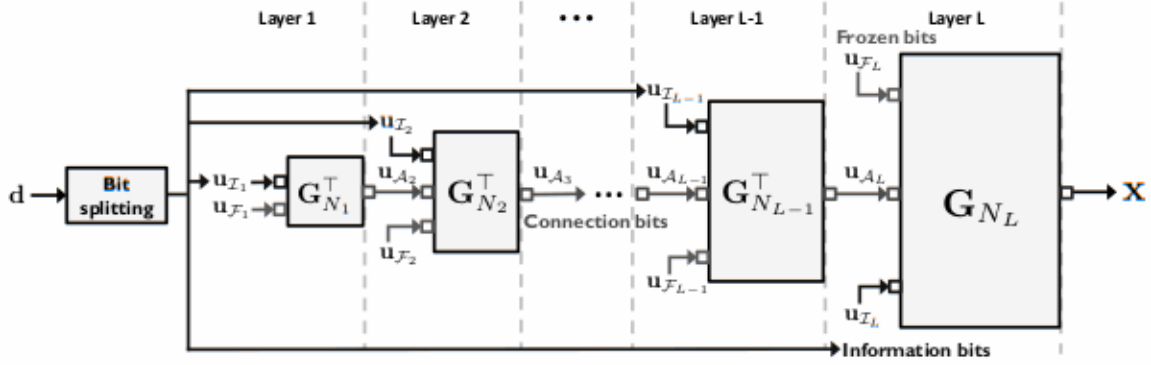


Fig. Fig. An illustration of the proposed deep polar encoder with layered layers.

that the weight of the soft-Godard equal while generating the pre-determined code weight distribution. The proposed rate-profiling method is to construct \mathcal{I}_ℓ and \mathcal{A}_ℓ for $\ell \in [L]$ individually across the layers,

Selections of \mathcal{I}_ℓ and \mathcal{A}_ℓ . We define \mathcal{I}_ℓ and \mathcal{A}_ℓ independently over the layers, suppose the channel input $x_\ell \in \{0, 1\}$ is formed by the transpose of polar transform $x_\ell = u_\ell \mathbf{G}_{N_\ell}^\top$, where i_1 is the index of the most reliable synthetic channel, for $\ell \in [1, 2, \dots, L-1]$ and the forward polar transform, i.e., $I(W_{N_\ell}^{(1)}) \geq I(W_{N_\ell}^{(2)}) \geq \dots \geq I(W_{N_\ell}^{(N_\ell)})$. This $x_L = u_L \mathbf{G}_{N_L}^\top$ for the last layer. Then, the codeword generated by layer ℓ encoder, x_ℓ , is assumed to be transmitted over an B-DMC, $W_\ell = \mathbf{X} \geq Z(W_\ell)$, which produces the channel values y_ℓ obtained from the density evolution when using layer approximation technique in [2], [2]. Using the ordered index set, the information set \mathcal{I}_ℓ is generated by selecting the bit-channel indices that are approximately polarized to the capacity of one for given code length N_ℓ :

$$\mathcal{I}_\ell = \left\{ i \in \mathcal{R}_\ell : I(W_{N_\ell}^{(i)}) \geq 1 - \delta_\ell \right\}, \quad (21)$$

where $i \in [N_\ell]$, $u_{\ell,a:b} = [u_{\ell,a}, u_{\ell,a+1}, \dots, u_{\ell,b}]$ for $a, b \in [N_\ell]$

where $\delta_\ell > 0$ is chosen arbitrarily small bit-channel K_ℓ capacity.

Next we construct the connection set \mathcal{A}_ℓ as a subset of $\mathcal{R}_\ell \setminus \mathcal{I}_\ell$ according to the RM rate-profiling. By selecting indices $[N_\ell]$ providing the highest bit-channel capacities in $\mathcal{R}_\ell \setminus \mathcal{I}_\ell$ larger than $I(W_{N_\ell}^{(i)}) \geq I(W_{N_\ell}^{(j)}) \geq \dots \geq I(W_{N_\ell}^{(N_\ell)})$, i.e., $I(W_{N_\ell}^{(j_{N_\ell-1})})$. Then,

$$\mathcal{R}_\ell = \left\{ i \in [N_\ell] : \text{wt}(\mathbf{g}_{N_\ell, i}) \geq d_\ell^{\min} \right\}, \quad (22)$$

$$\mathcal{A}_\ell = \{j_1, j_2, \dots, j_{N_\ell-1}\}, \quad (23)$$

where d_ℓ^{\min} is a target minimum distance for the ℓ th layer. The frozen set of layer ℓ is defined as the collection of indices that are excluded in both the information and connection sets as

$$\mathcal{R}_\ell = \{i_1, i_2, \dots, i_{|\mathcal{R}_\ell|}\}, \quad (23)$$

where i_1 is the index of the most reliable synthetic channel, i.e., $I(W_{N_\ell}^{(i_1)}) \geq I(W_{N_\ell}^{(i_2)}) \geq \dots \geq I(W_{N_\ell}^{(i_{|\mathcal{R}_\ell|})})$. This rate-profiling method is performed independently over the layers.

Remarks The rate-profiling method is based on the Bhattacharyya values, i.e., $Z(W_{N_\ell}^{(i_1)}) \leq Z(W_{N_\ell}^{(i_2)}) \leq \dots \leq Z(W_{N_\ell}^{(i_{|\mathcal{R}_\ell|})})$ or the values obtained from the density evolution with the same remarks about the coding complexity, [2]. The properties of the proposed method in terms of the information set, the generation of the CRC codes, and the rate-encoding capability are

Encoding complexity. The proposed type of successive decoding of L layers requires to take L polar transformations, each with N_ℓ size. Since the computation of the polar transform with size N_ℓ needs the complexity of $\mathcal{O}(N_\ell \log_2 N_\ell)$, the total encoding complexity boils down to where $\delta_\ell > 0$ is chosen arbitrary small and $|\mathcal{I}_\ell| = K_\ell$.

Next, we construct the connection set \mathcal{A}_ℓ as a subset of $\mathcal{R}_\ell \setminus \mathcal{I}_\ell$. Let $j_1, j_2, \dots, j_{N_\ell-1} \in \mathcal{R}_\ell \setminus \mathcal{I}_\ell$ be the indices that provide the highest N_ℓ bit-channel capacities in $\mathcal{R}_\ell \setminus \mathcal{I}_\ell$ such that $I(W_{N_\ell}^{(j_1)}) \geq I(W_{N_\ell}^{(j_2)}) \geq \dots \geq I(W_{N_\ell}^{(j_{N_\ell-1})})$ comparable to that of the standard polar codes when N_ℓ is sufficiently larger than N_ℓ for $\ell \in [L-1]$. Choosing a small size of N_ℓ for $\ell \in [L-1]$ is a practical and effective strategy for reducing the encoding complexity. The frozen set of layer ℓ is defined as the collection of indices $\mathcal{R}_\ell = \{i_1, i_2, \dots, i_{|\mathcal{R}_\ell|}\}$.

Superposition codes. The deep polar code can be viewed with action sets as superposition code of both the polar and the transformed polar codes as

$$\mathcal{F}_\ell = [N_\ell] / \{\mathcal{I}_\ell \cup \mathcal{A}_\ell\}. \quad (26)$$

$$\mathbf{x} = \underbrace{\sum_{j \in \mathcal{I}_\ell} u_{\ell,j} \mathbf{g}_{N_\ell, j}}_{\mathbf{x}_P} + \underbrace{\sum_{i \in \mathcal{A}_\ell} u_{\ell,i} \mathbf{g}_{N_\ell, i}}_{\mathbf{x}_{TP}}. \quad (27)$$

Remarks where \mathbf{x}_P and \mathbf{x}_{TP} represent polar and pre-transformed polar subwords, respectively. This superposition property, the superposition provides a useful guideline for designing a low-complexity decoder while improving the weight distribution. Specifically, the pre-transformed subcodewords play a crucial role in improving the weight distribution of the deep polar encoder. The polar subcodewords requires to take L polar decoding because each with N_ℓ size. Since the computation of the polar transform with size N_ℓ needs the complexity of $\mathcal{O}(N_\ell \log_2 N_\ell)$ the total encoding complexity boils down to

the deep polar codes offer a desirable balance between code performance and decoding complexity by strategically allocating information bit sizes between $N_{\ell+1}$ and N_ℓ . For instance, when the blocklength goes to infinity, the encoder allocates all information bits to $u_{\ell,1}$ while $\mathcal{A}_\ell = \emptyset$; the deep polar codes boil down to a standard polar code. It is worth mentioning that the encoding complexity can be comparable to that of the standard polar codes when N_ℓ is sufficiently large and N_ℓ weight distribution minimizes the distance of the deep polar codes is large and effective strategy for reducing the encoding complexity construction,

the superpositions codes shown in Fig. 10 can be viewed with a lens of length L through a superposition code of both the polar and the transformed polar codes as

$$\text{wt}(g_{N_L, j}) \geq d_L^{\min} \quad (29)$$

for $j \in \mathcal{I}_{L \cup \mathcal{A}_L}$. Since the pre-transform matrix of layer $L-1$ holds the upper triangular structure, the minimum distance of the pre-transformed subcodewords $\mathbf{x}_{\text{TP}} = \sum_{i \in \mathcal{A}_L} u_{L,i} g_{N_L,i}$, where \mathbf{x}_0 is a vector with all entries zero, is equal to the minimum distance of the polar code.

CRC-and (CA) deep polar codes. One possible extension of deep polar codes is to concatenate them with CRC low-complexity decoder while improving the weight distribution. Specifically, the K -bit information vector \mathbf{d} is pre-coded by using CRC generator polynomials, adding CRC play a crucial role in improving the weight distribution of bits. The length of the resulting information sequence becomes $K + K_{\text{CRC}}$, where K_{CRC} represents the number of CRC bits. Alternatively, multiple CRC bits, each with short length, can be appended to the information bits of each layer, i.e., u_2^e , when the connection bits u_1^e are treated as additional frozen bits. As a result, the deep polar codes offer a desirable balance between code performance and decoding discussed in the simulation section.

Rate-compatibility: A design of rate-compatible codes between u_L^L and u_L^A . For instance, when the blocklength suitable for hybrid automatic repeat request (HARQ) is L , the encoder allocates all information bits goes to infinity, the encoder allocates all information bits important feature for practical communication systems. Our to u_L^L , while $\mathcal{A}L = \phi$, the deep polar codes boil down to deep polar code possesses a rate-compatible property, thanks to a standard polar code.

The minimum distance and weight distribution: The transmitter sends a codeword \mathbf{x} and a receiver fails to decode the message bits \mathbf{d} . Then, in the next round of the transmission, or equal to the minimum distance of layer $L-1$, $d_{\mathbf{L}}^{min}$. By the transmitter sends only the output of $L-1$ layers, $\mathbf{u}_{\mathbf{L}}$, with construction, the encoder chooses the row vectors of $\mathbf{G}_{\mathbf{N}, \mathbf{L}}$, with blocklength of N_{L-1} for enabling HARQ communications with the weight larger than $d_{\mathbf{L}}^{min}$, namely,

The receiver attempts to decode the message by using both the noisy connection bits received in the second round and the received signal in the first round. This re-transmission and decoding protocol can be iteratively applied to the first layer, $L=1$, holding the upper triangular structure, the minimum distance from $\mathbf{R} = \frac{N_L}{N_L}$ to $\mathbf{R} = \sum_{l=L}^N \frac{N_l}{N_l}$. Notwithstanding the flexible rate compatibility, a delicate code optimization is required to aid the decoding performance. One possible extension of the bidependent polar codes is to incorporate them with CRC codes. In this approach, the K-bit information remains as promised by using 6 CRC generator polynomials, adding CRC bits. The length of the resulting information

In this section, we provide some examples of the design of deep polar with codes in a length, blocklength N , intended to better information about proposed underlying method. Throughout the examples, the decoding performance of the effects of CRC code on concatenating with the deep Polar code will be discussed in the simulation section at two different rates.

R Rate-compatibility: A design of rate-compatible codes suitable for hybrid automatic repeat request (HARQ) is an important feature for practical communication systems. Our deep polar code construction it is important to understand the polarized bit-channel capacities and the row weight of \mathbf{G}_2 . As shown in Fig. 22, the red circles indicate a bit-channel capacities for the BEC with $I(W) = 0.5$, i.e., bits $W_2^{(j)}$. Then j in [8]. The blue numbers indicate the normalized

transmitter sends only the output of $L-1$ layer, $\mathbf{u}_{\mathcal{A}_L}$, with blocklength of N_{L-1} for enabling HARQ communications. The receiver attempts to decode the message by using both the noisy connection bits received in the second round, and the received signal in the first round. This re-transmission and decoding protocol can be iteratively applied to the first layer, enhancing the decoding performance while reducing the code rates from $R = \frac{K}{N_L}$ to $R = \frac{K}{\sum_{\ell=1}^{L-1} N_\ell}$. Notwithstanding the flexible rate-compatibility, a delicate code optimization is required to attain a high HARQ performance by carefully choosing the blocklengths N_ℓ and information bits K_ℓ for each layer $\ell \in \{1, 2, \dots, L-1\}$. Solving this optimization problem remains as a promising future topic.

IV. EXAMPLES

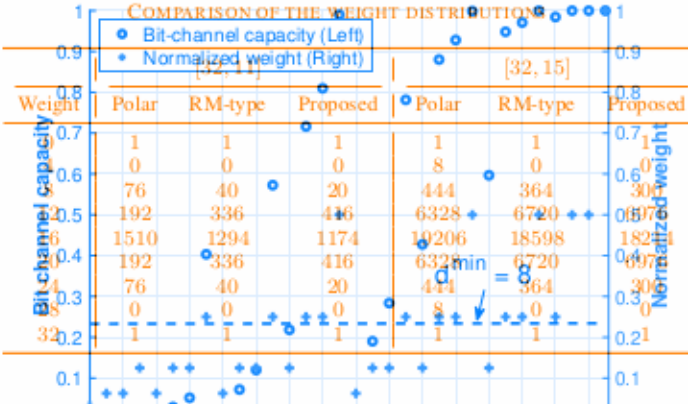
In this section, we provide some examples of the design of deep polar codes in a short blocklength regime to better understand the proposed encoding method. Throughout the examples, we shall focus on a short packet transmission scenario with a length of 32 over a BEC with an erasure probability of 0.5, i.e., $I(W) = 0.5$. The ordered index sets are mismatched according to bit-channel capacities and the normalized weights. For instance, $A \xrightarrow{\text{Channel Polarization}} B \xrightarrow{\text{Row Weights of } G_{32}}$. When including the bit-index 25 in the information set to facilitate SC decoding and then polarizing bit channels according to the easily weighted of IG become crucial to fully select the bit-indices that have the coding properties for this BEC with their weights, i.e., the bit-channel capacities [32]. The blue cross indicates the normalized weight of G_{32} according to *Example 1*, i.e., $\frac{\text{wt}(g_{32,i})}{32}$. The ordered index sets are mismatched due to the coupling between bit capacities and deep polarized weights. For instance, $B \xrightarrow{\text{Encoding Process}} A$. The encoding process involves utilizing two transformation matrices: G_1^\top for layer 1 but G_2^\top for layer 2. Assuming that a target minimum distance of the second layer is $d_2^{\min} = 8$, we select the indices of rows in the matrix G_{32} , whose weights are greater than or equal to $d_2^{\min} = 8$, i.e., $K_2 = \{8, 12, 14, 15, 16, 20, 22, 23, 24, 26, 27, 28, 29, 30, 31, 32\}$.

B. Example 1
 Then, from Fig. ??, the information set for the second layer, \mathcal{R}_2 , is chosen as
 This example explains how to construct a two-layered deep polar code with a code rate of $R = \frac{11}{32}$. The encoding process involves utilizing two transformation matrices: \mathbf{G}_8^\top for layer 1 and \mathbf{G}_{32}^\top for layer 2. Assuming that a target minimum distance of the second layer is $d_2^{\min} = 8$, we select the indices of rows in the matrix \mathbf{G}_{32} whose weights are greater than or equal to $d_2^{\min} = 8$, i.e., the eight bit-channel indices that yield the highest capacity in $\mathcal{R}_2 \setminus \{8, 13, 14, 15, 16, 20, 22, 23, 24, 26, 27, 28, 29, 30, 31, 32\}$.

Then, from Fig. 22, the information set for the second layer, a subset of \mathcal{R}_2 , is chosen as

It is worth mentioning that the bit-channel index of 25 was excluded in the connection set although its capacity is larger than that of the index of 32, 31, 30, 28, 24, 16 ($W_{32}^{(12)}$), $\geq I(W_{32}^{(12)})$.

TABLE I



This is because $\text{wt}(g_{32,25}) = 4 < \text{wt}(g_{32,12}) = 8$. The frozen set of the second layer becomes

Bit index

Fig. 2. Polarized bit-channel capacity (left) and normalized weight (right) for the BEC with $I(W) = 0.5$. In the first layer, we identify the four indices that result in the highest bit-channel capacity using the polar transform matrix G_8^\top , while ensuring that the minimum distance d_{\min}^{min} is greater than or equal to 4. The corresponding information and frozen sets are chosen as $\mathcal{I}_2 = \{1, 2, 3, 5\}$ and $\mathcal{F}_1 = \{8, 7, 6, 4\}$, respectively. The output vector of the first layer, denoted as

Weight Polar RM-type Proposed Weight Polar RM-type Proposed

$v_1 = u_1 G_8^\top$ is then connected to the input of connection set

$u_{A_2} = v_1$

$u_{A_4} = v_1$

$u_{A_8} = v_1$

$u_{A_{16}} = v_1$

$u_{A_{32}} = v_1$

$u_{A_{64}} = v_1$

$u_{A_{128}} = v_1$

$u_{A_{256}} = v_1$

$u_{A_{512}} = v_1$

$u_{A_{1024}} = v_1$

$u_{A_{2048}} = v_1$

$u_{A_{4096}} = v_1$

$u_{A_{8192}} = v_1$

$u_{A_{16384}} = v_1$

$u_{A_{32768}} = v_1$

$u_{A_{65536}} = v_1$

$u_{A_{131072}} = v_1$

$u_{A_{262144}} = v_1$

$u_{A_{524288}} = v_1$

$u_{A_{1048576}} = v_1$

$u_{A_{2097152}} = v_1$

$u_{A_{4194304}} = v_1$

$u_{A_{8388608}} = v_1$

$u_{A_{16777216}} = v_1$

$u_{A_{33554432}} = v_1$

$u_{A_{67108864}} = v_1$

$u_{A_{134217728}} = v_1$

$u_{A_{268435456}} = v_1$

$u_{A_{536870912}} = v_1$

$u_{A_{1073741824}} = v_1$

$u_{A_{2147483648}} = v_1$

$u_{A_{4294967296}} = v_1$

$u_{A_{8589934592}} = v_1$

$u_{A_{17179869184}} = v_1$

$u_{A_{34359738368}} = v_1$

$u_{A_{68719476736}} = v_1$

$u_{A_{137438953440}} = v_1$

$u_{A_{274877856800}} = v_1$

$u_{A_{549755713600}} = v_1$

$u_{A_{1099511427200}} = v_1$

$u_{A_{2199022854400}} = v_1$

$u_{A_{4398045708800}} = v_1$

$u_{A_{8796091417600}} = v_1$

$u_{A_{17592182835200}} = v_1$

$u_{A_{35184365670400}} = v_1$

$u_{A_{70368731340800}} = v_1$

$u_{A_{140737462681600}} = v_1$

$u_{A_{281474925363200}} = v_1$

$u_{A_{562949850726400}} = v_1$

$u_{A_{1125899701452800}} = v_1$

$u_{A_{2251799402905600}} = v_1$

$u_{A_{4503598805811200}} = v_1$

$u_{A_{9007197611622400}} = v_1$

$u_{A_{1801439522324800}} = v_1$

$u_{A_{3602879044649600}} = v_1$

$u_{A_{7205758089299200}} = v_1$

$u_{A_{14411516178598400}} = v_1$

$u_{A_{28823032357196800}} = v_1$

$u_{A_{57646064714393600}} = v_1$

$u_{A_{11529212928778400}} = v_1$

$u_{A_{23058425857556800}} = v_1$

$u_{A_{46116851715113600}} = v_1$

$u_{A_{92233703430227200}} = v_1$

$u_{A_{184467406860454400}} = v_1$

$u_{A_{368934813720908800}} = v_1$

$u_{A_{737869627441817600}} = v_1$

$u_{A_{147573925488363200}} = v_1$

$u_{A_{295147850976726400}} = v_1$

$u_{A_{590295701953452800}} = v_1$

$u_{A_{1180591403906905600}} = v_1$

$u_{A_{2361182807813811200}} = v_1$

$u_{A_{4722365615627622400}} = v_1$

$u_{A_{9444731231255244800}} = v_1$

$u_{A_{18889462462510489600}} = v_1$

$u_{A_{37778924925020979200}} = v_1$

$u_{A_{75557849850041958400}} = v_1$

$u_{A_{15111569970083916800}} = v_1$

$u_{A_{30223139940167833600}} = v_1$

$u_{A_{60446279880335667200}} = v_1$

$u_{A_{120892559760671334400}} = v_1$

$u_{A_{241785119521342668800}} = v_1$

$u_{A_{483570239042685337600}} = v_1$

$u_{A_{967140478085370675200}} = v_1$

$u_{A_{1934280956170741350400}} = v_1$

$u_{A_{3868561912341482700800}} = v_1$

$u_{A_{7737123824682965401600}} = v_1$

$u_{A_{15474247649365930803200}} = v_1$

$u_{A_{30948495298731861606400}} = v_1$

$u_{A_{61896990597463723212800}} = v_1$

$u_{A_{123793981194927446425600}} = v_1$

$u_{A_{247587962389854892851200}} = v_1$

$u_{A_{495175924779709785702400}} = v_1$

$u_{A_{990351849559419571404800}} = v_1$

$u_{A_{1980703691118839142809600}} = v_1$

$u_{A_{3961407382237778285619200}} = v_1$

$u_{A_{7922814764475556571238400}} = v_1$

$u_{A_{15845629328951113142476800}} = v_1$

$u_{A_{31691258657852226284953600}} = v_1$

$u_{A_{63382517315704452569887200}} = v_1$

$u_{A_{12676503463540890513774400}} = v_1$

$u_{A_{25353006927081781027548800}} = v_1$

$u_{A_{50706013854163562055097600}} = v_1$

$u_{A_{10141202770832712411019200}} = v_1$

$u_{A_{20282405541665424822038400}} = v_1$

$u_{A_{40564811083330849644076800}} = v_1$

$u_{A_{81129622166661699288153600}} = v_1$

$u_{A_{162259244333233998576307200}} = v_1$

$u_{A_{324518488666467997152614400}} = v_1$

$u_{A_{649036977332935994305228800}} = v_1$

$u_{A_{129807395466587198671055600}} = v_1$

$u_{A_{259614790933174397342111200}} = v_1$

$u_{A_{519229581866348794684222400}} = v_1$

$u_{A_{103845916373269598936844800}} = v_1$

$u_{A_{207691832746539197873689600}} = v_1$

$u_{A_{415383665493078395747379200}} = v_1$

$u_{A_{830767330986156791494758400}} = v_1$

$u_{A_{166153466197231358298911200}} = v_1$

$u_{A_{332306932394462716597822400}} = v_1$

$u_{A_{664613864788925433195644800}} = v_1$

$u_{A_{132922772977785866639128800}} = v_1$

$u_{A_{265845545955571733278257600}} = v_1$

$u_{A_{531691091911143466556515200}} = v_1$

$u_{A_{106338218382226893311303200}} = v_1$

$u_{A_{212676436764453786622606400}} = v_1$

$u_{A_{425352873528907573245212800}} = v_1$

$u_{A_{850705747057815146490425600}} = v_1$

$u_{A_{1701411494115630292980851200}} = v_1$

$u_{A_{3402822988231260585961702400}} = v_1$

$u_{A_{6805645976462521171923404800}} = v_1$

$u_{A_{1361129195292542234386809600}} = v_1$

$u_{A_{2722258390585084468773619200}} = v_1$

$u_{A_{5444516781170168937547238400}} = v_1$

$u_{A_{1088903562340337875094476800}} = v_1$

$u_{A_{2177807124680675750188953600}} = v_1$

$u_{A_{4355614249361351500377871200}} = v_1$

$u_{A_{8711228498722703000755742400}} = v_1$

$u_{A_{1742245697744540600151488000}} = v_1$

$u_{A_{3484491395489081200302960000}} = v_1$

$u_{A_{6968982790978162400605920000}} = v_1$

$u_{A_{1393796558195632800121840000}} = v_1$

$u_{A_{2787593116391265600243680000}} = v_1$

$u_{A_{5575186232782531200487360000}} = v_1$

$u_{A_{1115037246565066400974720000}} = v_1$

$u_{A_{2230074493130132801949440000}} = v_1$

$u_{A_{4460148986260265603898880000}} = v_1$

$u_{A_{8920297972520531207797760000}} = v_1$

$u_{A_{1784059594504106241559520000}} = v_1$

$u_{A_{3568119189008212483119040000}} = v_1$

$u_{A_{7136238378016424966238080000}} = v_1$

$u_{A_{14272476756032849932476160000}} = v_1$

$u_{A_{28544953512065699864952320000}} = v_1$

$u_{A_{57089867024131399729874640000}} = v_1$

$u_{A_{11417934404826279455749280000}} = v_1$

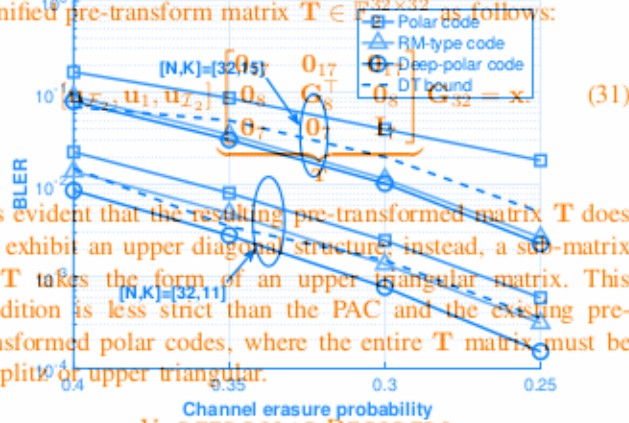
$u_{A_{22835868809652558911498560000}} = v_1$

$u_{A_{45671737619305117822997120000}} = v_1$

$u_{A_{91343475238610235645994240000}} = v_1$

$u_{A_{18268695047722047129198480000}} = v_1$

instance, we express our two-layered encoding structure with a unified pre-transform matrix $\mathbf{T} \in \mathbb{R}^{32 \times 32}$ as follows:



It is evident that the resulting pre-transformed matrix \mathbf{T} does not exhibit an upper diagonal structure; instead, a sub-matrix of \mathbf{T} takes the form of an upper triangular matrix. This condition is less strict than the PAC and the existing pre-transformed polar codes, where the entire \mathbf{T} matrix must be Toeplitz or upper triangular.

V. DEEP POLAR DECODERS

In this section, we present two decoding algorithms for deep polar codes. The first decoding method is SCL with backpropagation to parity check (SCL-BPC), which although having no polar balancing complexity and performance mismatch among distance control, deep polarized by the lighter position code interpretation, the by conducting the forward path, still the mechanism to weight the decoding latency at the cost increased hardware complexity. One remarkable result is that the deep polar codes can achieve better BLER performances than the SCL-BPC Decoder. The central concept behind the SCL-BPC is to efficiently prune decoding paths that fail to satisfy the successive parity check equation. Pre-transform using a sub-upper triangular SCL testing process. As a companion step toward understanding the mechanism, it is instructive to examine the BPC mechanism over restating previous information gain across the proposed layers. At the seen as a submatrix of BPC mechanism as matrix. For instance, we express our two-layered encoder from (27) with a unified pre-transform matrix connection bits of layerwise $\mathbf{G}_{N_{\ell-1}}^T$, \mathbf{u}_{A_ℓ} , using the input of encoder at layer $\ell - 1$ and $\mathbf{G}_{N_{\ell-1}}^T$ as

$$[\mathbf{u}_{A_\ell}, \mathbf{u}_{I_2}, \mathbf{u}_{I_2}] \begin{bmatrix} 0_{17} & 0_{17} & 0_{17} \\ 0_8 & \mathbf{G}_{N_{\ell-1}}^T & \mathbf{u}_{I_2} \\ 0_7 & 0_7 & I_7 \end{bmatrix} \mathbf{G}_{32} = \mathbf{x}. \quad (31)$$

From this successive encoder structure, we know that if \mathbf{u}_{A_ℓ} is successfully decoded, the reverse encoding using $\mathbf{T}_{\ell-1}^{-1} = \mathbf{G}_{N_{\ell-1}}^T$ ensures that the resulting pre-transformed matrix \mathbf{T} does not exhibit an upper diagonal structure; instead, a sub-matrix of $\mathbf{T}_{\ell-1} = (\mathbf{u}_{A_\ell} \mathbf{G}_{N_{\ell-1}}^T)$ takes the form of an upper triangular matrix. This condition is less strict than the PAC and the existing pre-transformed polar codes, where the entire \mathbf{T} matrix must be Toeplitz or upper triangular. Precisely estimating \mathbf{u}_{A_ℓ} is crucial for effective decoding using the BPC mechanism. However, accurately estimating the connection bits in layer L presents a significant challenge due to their transmission over less reliable bit channels with the information decoding during SCLs decoding. Consequently, the first decoding method can SCL with degradation in the parity check (SSCL-BPC), which partly violates flexibility in insufficient memory and performance. We propose an efficient SCL-BPC decoder hyperposing a bit-interleaved BPC mechanism secondarily with the standard polar SCL which aims to reduce the decoding backpropagation cost of in the check function within each layer.

Algorithm 4: SCL-BPC Decoder

Data centralized concept behind SCL-BPC is to efficiently prune decoding paths that fail to satisfy the successive parity check equations with frozen bits in polar encoder due to the ESGL-based decoding process. As at stepping stone toward understanding the overall SCL-BPC decoder, it is instructive to explain the BPC mechanism used in decoding.

$P_{\text{alive}} \leftarrow \{1\}$; $P_{\text{pool}} \leftarrow 2S/\mathcal{L}_{\text{alive}}$; $\text{PM}[s] \leftarrow 0, \forall s \in [S]$. The key concept behind the BPC mechanism is to leverage the reverse process of the deep polar encoder. From (??), the deep polar encoder generates the connection bits of layer ℓ , $\mathbf{P}_{\text{alive}}$ doing the input of encoder at layer $\ell - 1$ and $\mathbf{G}_{N_{\ell-1}}$ as $\log \frac{p(\mathbf{y}, \hat{\mathbf{u}}_{L,1:i-1}[s] | u_{L,i}=0)}{p(\mathbf{y}, \hat{\mathbf{u}}_{L,1:i-1}[s] | u_{L,i}=1)}$.

$$\text{if } i \in \mathcal{F}_L \text{ then } // \text{ frozen bits} \\ \mathbf{u}_{A_\ell}^+ = [\mathbf{u}_{I_{\ell-1}}, \mathbf{u}_{A_{\ell-1}}, \mathbf{u}_{I_{\ell-1}}] \mathbf{G}_{N_{\ell-1}}. \quad (32)$$

From this successive encoder structure, we know that if \mathbf{u}_{A_ℓ} is successfully decoded, the reverse encoding using $\mathbf{T}_{\ell-1}^{-1} = \mathbf{G}_{N_{\ell-1}}^T$ copies the path produced by the frozen bits of the previous layer $P_{\text{alive}} \leftarrow P_{\text{alive}} \cup \{s'\}; P_{\text{pool}} \leftarrow P_{\text{pool}} / \{s'\}$

$$\hat{u}_{L,i}[s] \leftarrow 0; \hat{u}_{L,i}[s'] \leftarrow 1; \\ \text{PM}[s] \leftarrow \text{PM}[s] + \log(1 + e^{-(1-2\hat{u}_{L,i}[s])\eta_i}) \quad (33)$$

for $\ell \in \{2, 3, \dots, L\}$. Precisely estimating \hat{u}_{A_ℓ} is crucial for effective decoding using the BPC mechanism. However, accurately estimating the connection bits in layer L presents a significant challenge due to their transmission over less reliable bit channels than the information bits during SCL decoding. Consequently, incorrect estimation of \hat{u}_{A_ℓ} can lead to a degradation in the performance of SCL decoding, mainly when the list size is insufficiently large. If $\hat{u}_{F_{\ell-1}:k} \neq 0$ for some ℓ then Kill the path.

We propose an efficient SCL-BPC decoder by leveraging a bit-wise BPC $P_{\text{alive}} \leftarrow P_{\text{alive}} / \{s\}; P_{\text{pool}} \leftarrow P_{\text{pool}} / \{s\}$. The major idea is to verify the backpropagation syndrome check condition at the bit level within each layer, specifically for the elements denoted as $u_{L,i}$, where i belongs to the set A_L . To simplify our notation, we define $\mathbf{G}_{N_{\ell-1},1:k} \in \mathbb{R}^{32 \times k}$ as the upper-left submatrix of $\mathbf{G}_{N_{\ell-1}}$. It is important to note that our pre-transform technique using the polar transform matrix possesses a unique property: its inverse is equal to itself. As a result, the inverse pre-transformation matrix is simply calculated if set as $(\mathbf{G}_{N_{\ell-1},1:k})^{-1} = \mathbf{G}_{N_{\ell-1},1:k}$, $\forall \ell \in [L-1], \forall k \in [K]$.

If we denote the connection bits of layer ℓ as $\hat{u}_{A_\ell} = [\hat{u}_{\ell,1}, \hat{u}_{\ell,2}, \dots, \hat{u}_{\ell,N_{\ell-1}}]$ such that $i_1 < i_2 < \dots < i_{N_{\ell-1}}$, we express

$$*** \text{Information bits extraction} *** \\ \text{for } \ell = L, \dots, 2 \text{ do } \hat{u}_{\ell,1:k} = \hat{u}_{A_\ell,1:k} \mathbf{G}_{N_{\ell-1},1:k} \quad (35)$$

where $\hat{u}_{\ell-1}[s_k^*]$ is a subsequence that comprises the first k elements of $\hat{u}_{\ell-1}$. Next, we extract two portions from the estimated bits ($\hat{u}_{\ell-1}$ of layer $\ell-1$): one portion is used for parity checking, and the other portion consists of connection bits that are recursively applied using (??). Finally, we gather the estimated frozen bits from each

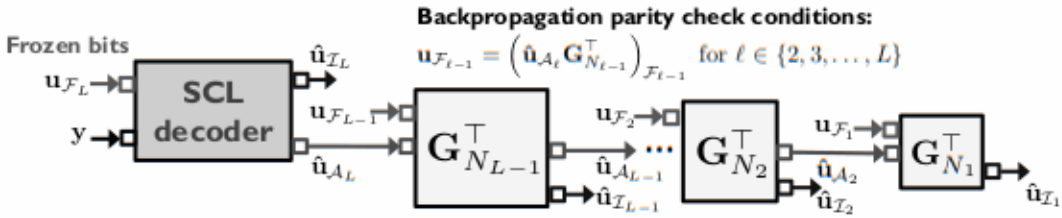


Fig. 4 FigA4 illustrates the SCL decoder using the backpropagation parity check principle.

specifically [1] or the denoted syndromes as depicted in Fig. ?? to the set \mathcal{A}_L . To simplify our notation, we define \mathbf{G} leveraging this bit-wise BPC mechanism, the proposed SCL decoder employs our pre-transforms by utilizing the polar transform. A key property of \mathbf{G} is the inverse of the code itself. As a consequence, the decoding is simply path selection of its binary tree and appending either $u_{L,i} = 0$ or $u_{L,i} = 1$ to each candidate path. Consequently, the number of paths is doubled [but limited to a predetermined maximum value S . In contrast to the standard SCL decoder, it is included in the list whenever a new path satisfies the BPC and ranks among the S most reliable paths. Conversely, it is discarded if a new path fails the BPC or exhibits lower reliability than the existing S paths in the list. This iterative process continues until $i \in [N_L]$. Ultimately, the decoder selects the path where $u_{\ell=1,1,k}$ is a subsequence that comprises the first k with the highest reliability metric as the output. When $S = 1$, our decoder simplifies to the SC decoder utilizing estimated bits $u_{\ell=1}$ of layer $\ell = 1$; one portion is used for the backpropagation parity check. The deep polar SCL decoding procedure is summarized in Algorithm ??.

The proposed decoder introduces an extra decoding complexity due to the BPC operation compared to the standard SCL decoding complexity with a list size of S , which is $\mathcal{O}(SN_L \log N_L)$. For each layer $\ell \in \{1, 2, \dots, N_L - 1\}$, the parity check can be performed with a complexity of $\mathcal{O}(N_\ell \log N_\ell)$. Consequently, the overall extends the list of candidate paths by exploring both paths of complexity is the sum of the complexity required for SCL binary tree and appending either $u_{L,i} = 0$ or $u_{L,i} = 1$ decoding and computing the inverse of the pre-transforms to each candidate path. Consequently, the number of paths is doubled but limited to a predetermined maximum value S . In contrast to the standard SCL¹ decoder, it is included in the list whenever a new path satisfies the BPC and ranks among the S most reliable paths. Conversely, it is discarded if it is not part of the S paths in the list. This iterative process continues until N_L significantly. Unlike the N_L decoder [2], the path with the highest reliability metric as the output. When $S = 1$, our decoder simplifies to the SC decoder utilizing the backpropagation parity check. The decoding complexity of the proposed SCL decoder is $\mathcal{O}(SN_L \log N_L) + \mathcal{O}(S(N_L \log N_L))$ compared to the standard SCL decoder in parallel decoding mode. The proposed SCL decoder is more complex than the standard SCL decoder due to the additional complexity introduced by the backpropagation parity check. The overall complexity of the proposed SCL decoder is $\mathcal{O}(2^{K-K_L} SN_L \log N_L)$.

If the complexity required for SCL decoding and the putting bits in the last layer transfer, the SCL decoder identifies the most reliable information vector from a list of size S . Denoting the result of SCL decoding for the j th possible connection bit pattern and frozen bits as $\hat{\mathbf{u}}_{I_L}^j$, the decoder selects the most reliable estimate $\hat{\mathbf{u}}_{I_L}^*$ for the information vector from the set $\{1, 2, \dots, 2^{K-K_L}\}$.

$$j = \arg \max_{j \in \{1, 2, \dots, 2^{K-K_L}\}} \log p(\mathbf{y}_L | \mathbf{u}_{F_L}, \mathbf{u}_{A_L}, \hat{\mathbf{u}}_{I_L}^j). \quad (37)$$

B. A Low-Latency Decoder

We also present a method for achieving low latency decoding by deep polar coding. Our approach involves parallel processing. Standard SCL decoders have a complexity of $\mathcal{O}(2^{K-K_L} SN_L \log N_L)$, which increases exponentially with the number of bits in a layer, K_L , as they are encoded in a frozen set alongside with $\{1, 2, \dots, 2^{K-K_L}\}$ and \mathbf{u}_{I_L} . There are 2^K possible connection bit patterns, and this method is limited to scenarios where the number of $K - K_L$ is small, where $j \in \{1, 2, \dots, 2^{K-K_L}\}$. Given the j th connection bit pattern $\mathbf{u}_{A_L}^j$ and the frozen bits of the last layer $\mathbf{u}_{F_L} = 0$, the SCL decoder identifies the most reliable information vector from a list of size S . Denoting the result of SCL decoding for the j th possible SCL decoding frozen bits as $\hat{\mathbf{u}}_{I_L}^j$, the decoder selects the most reliable estimate $\hat{\mathbf{u}}_{I_L}^j$ through the information vector from the highest $(1, 2, \dots, 2^{K-K_L})$ under the premise that the actual connection bits are utilized as the frozen bits. Therefore, $p(\mathbf{y}_L | \mathbf{u}_{F_L}, \mathbf{u}_{A_L}^j, \hat{\mathbf{u}}_{I_L}^j)$ needs to carefully optimize the list size and the number of parallel-SCL parallel SCL decoding methods to parallelize the deep polar SCL decoder by harnessing the power of parallel processing.

However, the hardware complexity of this method increases exponentially with the number of information bits encoded in \mathbf{u}_{I_L} . This section compares the BLERs of different encoding schemes. Consequently, practical usage of this method is limited to scenarios where the number of $K - K_L$ is small enough. In addition, the overall computational complexity of the parallel-SCL decoding becomes

$$\mathcal{O}(2^{K-K_L} S N_L \log N_L), \quad (38)$$

• Deep polar codes: We have developed deep polar codes with varying numbers of layers, $L \in \{2, 3, 4\}$, very based because the size of information bits may be chosen through the bit-chunk size with the highest expanding number. The figure shows that those four deep polar bits are assigned as the freezing bits. Therefore, in this implementation, the minimum weight of the list size and the code length of a parallel-SCL decoder with weight 2^{K-K_L} of this separable two of them. The proposed SCL decoder. This

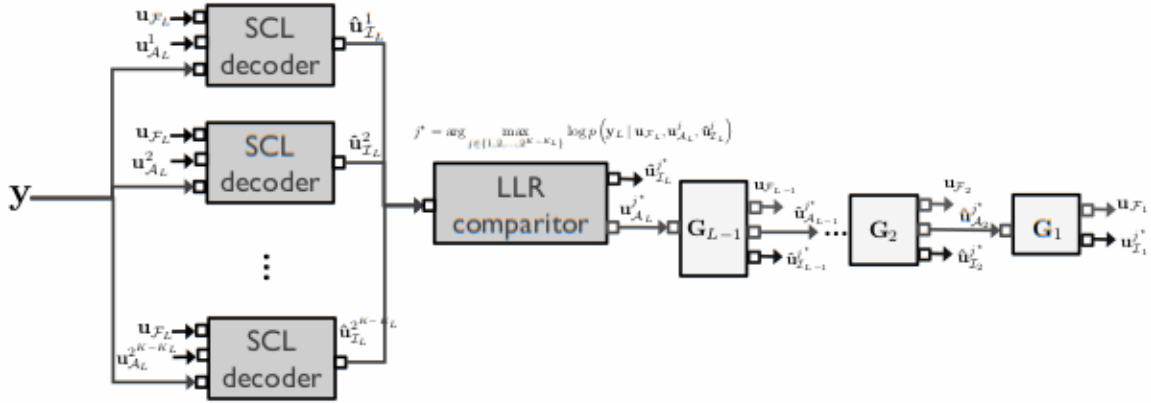


Fig. 5. The proposed block propagation decoding method using parallel SCL decoders.

observation. In Section 4, we show that multi-layered pre-transformations can increase the minimum distance of the code. This section compares the BLERs of different encoding and decoding methods under BI-AWGN channel.

- **CA-deep polar codes:** We employ CRC precoding as an extra pre-transformation before applying the successive deep polar encoding. We utilize the specific 6-bit CRC polynomial $1 + D^5 + D^6$ for the CRC precoding. We implement two types of deep polar codes with/without CRC precoding. The effectiveness of CRC precoding in enhancing the codes is demonstrated in Table ??.

Deep polar codes: We have developed deep polar codes where it is observed that the minimum distance is with varying numbers of layers, $L \in \{2, 3, 4\}$, based on increased with only a small number of layers for the size of the information bits K . For instance, Table ?? encoding. For example, the (128, 64) CA-deep polar shows encoding network configurations for deep polar code with two layers exhibits an increased minimum distance compared to the two-layered deep polar code without CRC precoding. This result suggests that CRC precoding serves as an additional pre-transformation that introduces more layers into the encoding process. Consequently, it contributes to the overall improvement in the performance of the deep polar codes.

- **CA-deep polar codes:** We employ CRC precoding as an extra pre-transformation before applying the successive deep polar encoding. We utilize the specific 6-bit CRC polynomial $1 + D^5 + D^6$ for the CRC precoding. The proposed SCL-BPC decoding and parallel-SCL decoding techniques with a list size of S , which are demonstrated in Table ??, where it is observed that the primarily utilized to reduce decoding complexity and minimum distance is increased with only a small number of layers during simulations. The ML decoding algorithm is also employed to gauge the gap-to-capacity deep polar code with two layers exhibits an increased performance specifically for low code rates, such as minimum distance compared to the two-layered deep polar code without CRC precoding. This result suggests that CRC precoding serves as an additional pre-transformation that introduces more layers into the encoding process.

We explain benchmark encoding and decoding schemes to compare the BLER performance in a short blocklength regime. The benchmarks are listed as follows:

- **Decoders:** We employ three decoding algorithms for the theoretical bounds [?]: We utilize the proposed SCL-BPC decoding scheme for the SCL decoding process employing list sizing M which specifically utilizes the dispersion and complexity and delays during the meta-converse analysis. The ML decoding algorithm is also employed.

to gauge the gap [?]. The specific performance is specifically for low code rates, calculated using the *Nsp* package, which can be accessed online at <https://github.com/Bpmit/spectre>.

These bounds allow us to demonstrate the gaps between the achievable performance of our methods and the upper bounds of the finite-blocklength capacity. The benchmarks are listed as follows:

- **CA-polar codes** [?]: The CA-polar codes serve as the baseline methods. The information sets are chosen according to the 5G standard specification in [?] when coding and decoding methods. Specifically, we plot the dispersion normal approximation and the meta-converse bounds for a given code length and rates, as described in $1 + D^5 + D^6$, which has shown the lowest BLER [?]. The dispersion and meta-converse bounds were calculated using the *spectre* package, which can be accessed online at <https://github.com/Bpmit/spectre>. These bounds allow us to demonstrate the gaps between the achievable performance of our methods and the upper bounds of the rate-profile algorithm and generator polynomials finite-blocklength capacity.
- **PAC codes** [?]: The PAC codes heavily depend on the performance of our methods and the upper bounds of the rate-profile algorithm and generator polynomials finite-blocklength capacity. The optimized rate-profiling method is known for information bit sizes of $K = 29$ baseline methods. The information sets are chosen according to the 5G standard specification in [?] when constructing the polar codes. In addition, we take into account the CRC precoding with the polynomial $c = 3211$ and $c = 133$ in the octal notation for $K = 29$ and $K = 64$, respectively.
- **CA-BOSS codes** [?]: We also consider comparing a CA-BOSS code with the CA-polar codes. For decoding block orthogonal sparse superposition (BOSS) code, the CA-polar codes we use the standard SCL decoder. Concatenating with CRC codes, the CA-BOSS code with a list size of S was shown to achieve the meta converse bounds [?].
- **PAC codes** [?]: The PAC codes heavily depend on the performance of our methods and the upper bounds of the rate-profile algorithm and generator polynomials finite-blocklength capacity. The optimized rate-profiling method is known for information bit sizes of $K = 29$ and $K = 64$ under blocklength of 128 [?]. Specifically, the PAC codes adopt the generator polynomials $c = 3211$ and $c = 133$ in the octal notation for $K = 29$ and $K = 64$, respectively.
- **CA-BOSS with PAC codes**: Fig. ?? presents the comparison of the BLER performance for the CA-BOSS and PAC codes. The CA-BOSS code with the CA-polar codes is optimized for the convolutional code. The optimized rate-profiling method is known for information bit sizes of $K = 29$ and $K = 64$ under blocklength of 128 [?]. Specifically, the PAC codes adopt the generator polynomials $c = 3211$ and $c = 133$ in the octal notation for $K = 29$ and $K = 64$, respectively.

Algorithm 1: SCL-BPC Decoder

DP for $s \in \mathcal{P}_{\text{alive}}$ do // path cloning Polar
 DP ?? $\eta_L \leftarrow \log \frac{p(128, 16)_1 | s \in \mathcal{G}_d, ?=0)}{p(256, 16)_1 | s \in \mathcal{G}_d, ?=1)}$ Polar
 CA-DP if ?? $\in \mathcal{F}_L$ them // frozen bits Polar + CRC6
 CA-DP ?? $\hat{u}_{L,i}[s] \in \{128, 16\}$; 5G [?]; Polar + CRC6
 CA-DP ?? $\hat{u}_{L,i}[s] \in \{256, 16\}$; 5G [?]; Polar + CRC6
 CA-polar ?? $\eta_L \leftarrow \text{PM}[s] + \text{PM}[s] + \log(1 + e^{-(1-2\hat{u}_{L,i}[s])\eta_L})$;
 else // information bits CRC6
 PAC ?? $\eta_L \leftarrow \log \frac{\sqrt{N} K}{s}$; 5G [?];
 PAC ?? $\eta_L \leftarrow \log \frac{(128, 64)}{(128, 64)} \cdot \text{RM}[?]$; CC [c] $\in \{32, 64\}$
 CC [c] $\in \{32, 64\}$
 ** DP: deep polar, DEGA: Density Evolution with Gaussian Approximation
 ** Estimate $d_L^{\text{ML}}[s] \leftarrow 0; u_L[s] \leftarrow -1$.
 $P_{\text{alive}} \leftarrow \text{alive} \cup \{s\}; P_{\text{pool}} \leftarrow P_{\text{pool}} / \{s\}$
 $\text{PM}[s] \leftarrow \text{PM}[s] + \log(1 + e^{-(1-2\hat{u}_{L,i}[s])\eta_L})$;
 $\text{PM}[s'] \leftarrow \text{PM}[s'] + \log(1 + e^{-(1-2\hat{u}_{L,i}[s'])\eta_L})$;
 implement a CA-BOSS code with the CRC polynomial of
 $1 + D + D^3$. We refer the reader to [?] for the construction
 end
 end
 details.
 If $i \in \mathcal{A}_L$ then // parity check

C. BLER for $s \in \mathcal{P}_{\text{one}}$ do

Apply inverse transform according to (??);

Comparison with PAC codes: Fig. ?? presents the comparisons of BLER performances among three coding schemes: deep polar codes, the PAC codes with optimized rate-profiling, and 5G standard CA-polar codes, each evaluated at two distinct code rates, $R \in \{ \frac{1}{2}, \frac{1}{3} \}$. The meta-converse and the normal approximation bounds are plotted as theoretical benchmarks for the corresponding code rates. For decoding, SCL-BPC decoders are utilized for deep polar codes, while SCL decoders are employed for both PAC and CA-polar codes with varying list sizes, $S \in \{8, 32, 256\}$. The solid lines on the graph correspond to the BLER performances of SCL-BPC and SCL decoders when using a short list size of $S = 8$. The results demonstrate that deep polar codes outperform PAC and CA-polar codes when employing a short list size, particularly where $R = \frac{1}{128}$, PAC codes exhibit a worse BLER performance than CA-polar codes. Additionally, we observe the dotted lines on the plot, representing the BLER performances with larger list sizes, i.e., $S = 32$ for $K = 29$ and $S = 256$ for $K = 64$. Notably, with sufficiently large list sizes, both deep polar and PAC codes closely achieve the normal approximation bound on white; CA-polar codes still exhibit a gap from the bound.

Comparison with 5G CA-polar codes: Fig. ?? illustrates the comparison of BLER performance between the proposed deep polar and 5G CA-polar codes using two decoding methods: SC and SCL with a list size of $S = 8$. The simulation results reveal that our deep polar codes consistently outperform

TABLE III
SIMULATION PARAMETERS

BLER meta-converse and the normal approximation bounds are plotted as theoretical benchmarks for the corresponding code rates. For decoding, SCL-BPC decoders are utilized for deep polar codes, while SCL decoders are employed for shallow polar codes. Both PAC and CA-polar codes with varying list sizes, $\ell \in [4]$, Decoder Design Estimate, $\ell = 1$, $\ell = 2$, $\ell = 3$, $\ell = 4$

The solid lines on the graph correspond to the BLER performances of SCL-BPC and SCL decoders when using a short list size of $S = 8$. The results demonstrate

using a short list size of 3 or 6. The results demonstrate that deep polar codes outperform PAC and CA-polar SCL codes when employing a short list size, particularly where

PAC codes exhibit a worse BLER performance than SCA-polar codes. Additionally, we observe the dotted

ML lines on the plot, representing the BLER performances

^{ML} with larger list sizes,³¹ i.e., $S = 32$ for $K = 29$ and $S = 256$ for $K = 64$. Notably, with sufficiently large list sizes,

ML both deep polar and PAC codes closely achieve the normal approximation bound, while CA-polar codes still exhibit

SCL Comparison with CA-polar codes: Fig. ?? illustrates the SCL gap from the bound.

SCL ¹⁶ on [2]. CC: Convolutional Coding
proposed deep polar and 5G CA-polar codes using two

decoding methods: SCL-BPC and SCL with a list size of $S = 8$. The simulation result reveals that our deep polar

$S = 8$. The simulation result reveals that our deep polar codes' consistent counterparts perform the CA polar rates, namely at three specific odd rates numerically $R = \{.32, .56, .96\}$.

This result suggests that the proposed deep polar code

the polar coiled-coil superhelical persistence length compared to the GsC superhelix performance is not comparable to the GsC superhelix performance while the polar coiled-coil superhelix exhibits a higher ratio, while the increase

Performance of parallel-SCT decoder: Fig. 22 shows the

Performance of parallel-SCL decoder. Fig. 11 shows the BER performance of parallel-SCL decoder (Agpolar

shows under $\text{PAC}_{\text{L}}^{\text{SCL}}$ the binding of the template to the PAC_{L} , SCL complex or to the $\text{PAC}_{\text{L}}^{\text{SCL}}$ complex. The $\text{PAC}_{\text{L}}^{\text{SCL}}$ complex is formed by the PAC_{L} and SCL proteins.

plement this paper a list of the corresponding general and CA-specific coders of information in the *K* patterns smallest before net bit indices at the generation $2^K - K$, parallel to Sections 6 of the preceding

patterns. Negligibly, we apply the padding bits decoded by reading bit gathered information of patterns bits pad patterns frozen, bits. Apply each possible frozen decod pattern by adding the appropriate

SIC decoding bit pattern sizes of addition The simulation results for shows possible propagation bit pattern performed CAE applies PACE

SQEs undergo growth with SCL due to decoding by S after 2. Then the initial transformation gives birth to new polar parallel SCLs percolating CA-polar and PA-polar clusters, the latter being SCLs due to decoding by T after 2.

and Fig. A.7 shows the BLRIT performance on the polar coding that directly prioritizes GCR and CA robustness by parallel-SCI. We design a parallel-SCI decoder with list size $S = 2$ to

Figure 2 shows the performance of the proposed deep polar channel equalizer (DEPCE) decoder with list size $L = 2$ to decode deep polar code BLER performance length of Kdeep29 polar bits decoded by parallel-SGL BinerRCA polar deep polar

SCL under parallel SCL and parallel SCL between them with CAT polar codes under SCL under parallel SCL size with message length $m = 16$

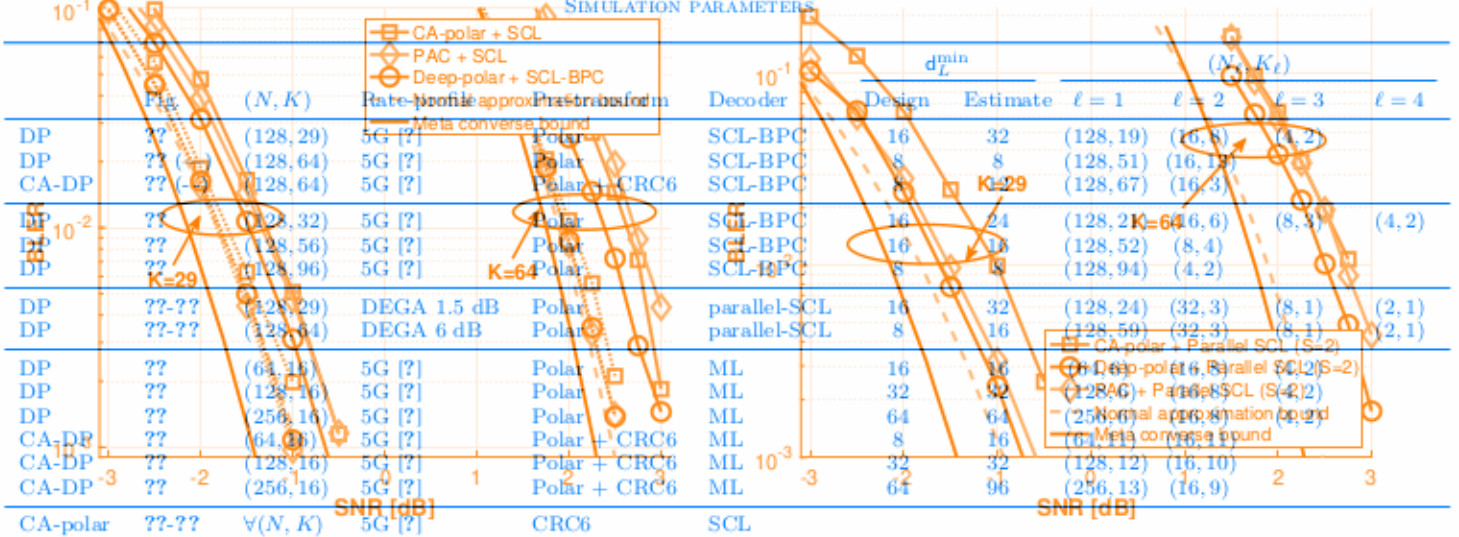
Lang32. Even if the total listsizes of computations K parallel SGEMM operations of deep neural networks under parallel like SGD does not exceed the size of lists of GEMM, including 1 toward the SGD

decoding operations to achieve low decoding latency by the early decoding with the listability of ddp, polarCode32 or even later by

total number of apertures of parallel-SCL is larger than SCL in comparison with A-B-BOSS codes [Figure 22] indicates the

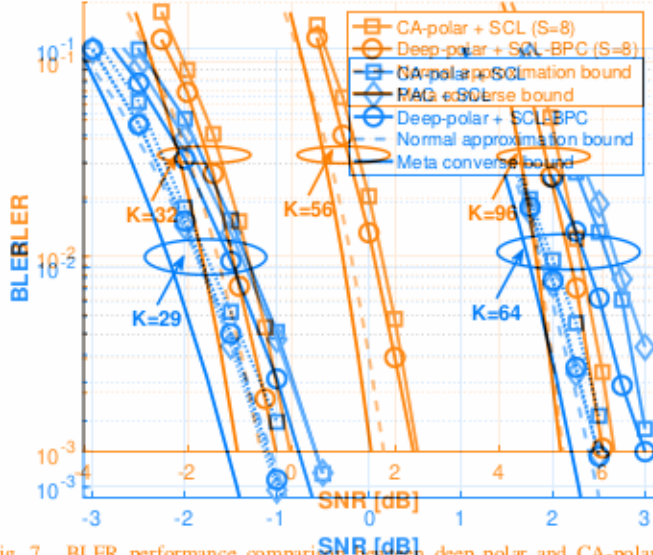
TABLE II

SIMULATION PARAMETERS

Fig. 6. BLER performance of PAC, CA-polar, and deep polar codes. Parameters for solid line are $(K, S) \in \{(29, 8), (64, 8)\}$, and for dotted line are $(K, S) \in \{(29, 32), (64, 256)\}$.

line and DEGA (K, S) = {(29, 8), (64, 8), (128, 16)}

Deep polar (K, S) = {(29, 8), (64, 8), (128, 16)}

** Estimate d_L^{\min} is computed using SCL(BPC) decoder with list size $S = 10^4$.Fig. 6. BLER performance of PAC, CA-polar, and deep polar codes. Parameters for solid line are $(K, S) \in \{(29, 8), (64, 8)\}$, and for dotted line are $(K, S) \in \{(29, 32), (64, 256)\}$.

polar codes, CA-deep polar codes, CA-BOSS codes, and CA-polar codes, at different code rates $R \in \{\frac{16}{256}, \frac{16}{128}, \frac{16}{64}\}$. The results demonstrate the effectiveness of the proposed codeword mapping in improving the code performance. By utilizing ML decoding, we propose the MIF decoding performance of the CA-BOSS scheme, which is comparable to the deep polar codes. The CA-BOSS code exhibits superior decoding performance compared to other codes, especially for higher code rates. The CA-deep polar code exhibits superior decoding performance compared to other codes, especially for higher code rates. The CA-polar code exhibits superior decoding performance compared to other codes, especially for higher code rates.

Fig. 8. BLER performance under parallel-SCL decoder.

SCL

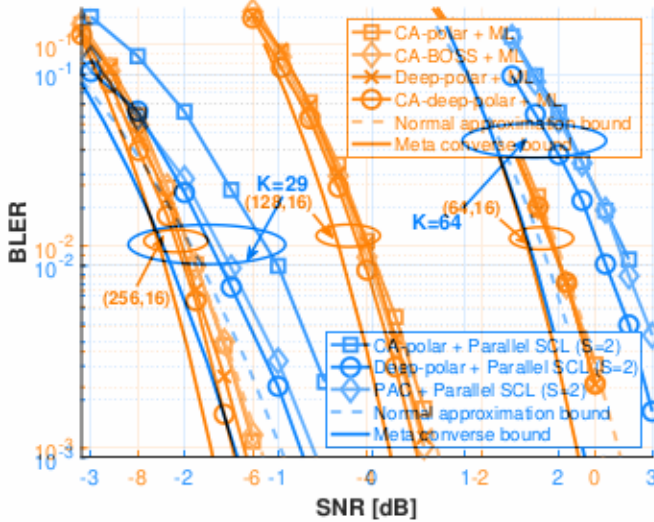


Fig. 10. BLER performance of deep polar, CA-deep polar, CA-polar, and CA-BOSS codes. The CRC polynomial is $1 + D^5 + D^6$ for CA-deep polar and CA-polar codes and $1 + D + D^3$ for CA-BOSS codes.

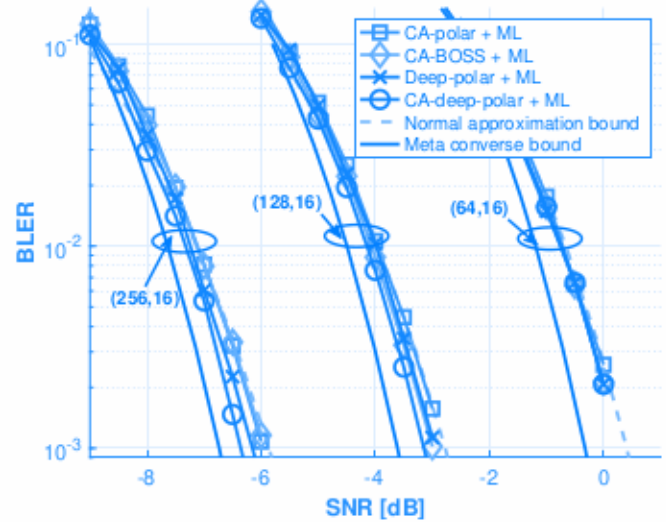


Fig. 10. BLER performance of deep polar, CA-deep polar, CA-polar, and CA-BOSS codes. The CRC polynomial is $1 + D^5 + D^6$ for CA-deep polar and CA-polar codes and $1 + D + D^3$ for CA-BOSS codes.

before. Our deep polar code is a superposition code of pre-transformed and regular polar subcodes. Controlling the rates of these two subcodes enables the design of low-complexity decoding while significantly improving the weight distribution of the codes. Leveraging this superposition property, we have also introduced two decoding methods: the SCL-BPC decoder, which effectively reduces decoding complexity, and the parallel-SCL decoder, which minimizes decoding latency. Through simulations, we have demonstrated that our codes achieve close to finite-blocklength capacity and consistently outperform all existing state-of-the-art pre-transformed polar codes at various rates and short blocklengths, all while maintaining a reasonable decoding complexity.

A promising further research direction would be to extend the deep polar code design to moderate blocklengths, such as up to 2048, in order to bridge the gap towards the finite-blocklength capacity in moderate blocklength regimes. Additionally, exploring the development of more efficient decoding algorithm for larger code blocklengths holds great promise, as the complexity of the SCL-BPC decoder may become computationally prohibitive in moderate blocklengths. Lastly, it is also interesting to design a rate-compatible deep polar code to optimally support HARQ protocols.

We have introduced a novel type of pre-transformed polar code called the deep polar code. The deep polar codes are generated through successive multi-layered encoding with a flexible rate-profiling method. The main technical innovation involves creating a unique yet universal pre-transformed architectures of polar codes, which is inspired by deep layered transform coding. These innovative architectures open up new possibilities for exploring a far more diverse range of pre-transformed polar code structures that were not explored before. Our deep polar code is a superposition code of pre-transformed and

regular polar subcodes. Controlling the rates of these two subcodes enables the design of low-complexity decoding while significantly improving the weight distribution of the codes. Leveraging this superposition property, we have also introduced two decoding methods: the SCL-BPC decoder, which effectively reduces decoding complexity, and the parallel-SCL decoder, which minimizes decoding latency. Through simulations, we have demonstrated that our codes achieve close to finite-blocklength capacity and consistently outperform all existing state-of-the-art pre-transformed polar codes at various rates and short blocklengths, all while maintaining a reasonable decoding complexity.

A promising further research direction would be to extend the deep polar code design to moderate blocklengths, such as up to 2048, in order to bridge the gap towards the finite-blocklength capacity in moderate blocklength regimes. Additionally, exploring the development of a more efficient decoding algorithm for larger code blocklengths holds great promise, as the complexity of the SCL-BPC decoder may become computationally prohibitive in moderate blocklengths. Lastly, it is also interesting to design an efficient rate-compatible deep polar code to optimally support HARQ protocols.